NUMERICAL LINEAR ALGEBRA WITH APPLICATIONS
Numer. Linear Algebra Appl. 2009; **16**:345–363
Published online 2 September 2008 in Wiley InterScience (www.interscience.wiley.com). DOI: 10.1002/nla.615

Preconditioning iterative algorithm for the electromagnetic scattering from a large cavity

Yingxi Wang, Kui Du and Weiwei Sun*, †

Department of Mathematics, City University of Hong Kong, Hong Kong

SUMMARY

A preconditioning iterative algorithm is proposed for solving electromagnetic scattering from an open cavity embedded in an infinite ground plane. In this iterative algorithm, a physical model with a vertically layered medium is employed as a preconditioner of the model of general media. A fast algorithm developed in (*SIAM J. Sci. Comput.* 2005; **27**:553–574) is applied for solving the model of layered media and classical Krylov subspace methods, restarted GMRES, COCG, and BiCGstab are employed for solving the preconditioned system. Our numerical experiments on cavity models with large numbers of mesh points and large wave numbers show that the algorithm is efficient and the number of iterations is independent of the number of mesh points and dependent upon the wave number. Copyright © 2008 John Wiley & Sons, Ltd.

Received 8 June 2007; Revised 20 June 2008; Accepted 21 June 2008

KEY WORDS: electromagnetic scattering; cavity; preconditioning iterative algorithm; Helmholtz equation; indefinite systems

1. INTRODUCTION

Electromagnetic scattering is one of the most competitive areas in both mathematical and engineering communities with a wide range of applications, such as astronomy, optics, meteorology, and remote sensing. In this paper, we are mainly concerned with electromagnetic scattering from two-dimensional large open cavities embedded in an infinite ground plane. The geometry is shown in Figure 1. The ground plane and the walls of the open cavity are perfect electric conductors (PEC), and the interior of the open cavity is filled with non-magnetic materials that may be inhomogeneous. The half-space above the ground plane is filled with a homogeneous, linear, and isotropic

*Correspondence to: Weiwei Sun, Department of Mathematics, City University of Hong Kong, Kowloon, Hong Kong.
†E-mail: maweiw@math.cityu.edu.hk

Contract/grant sponsor: Research Grants Council of the Hong Kong Special Administrative Region, China; contract/grant number: CityU 102204

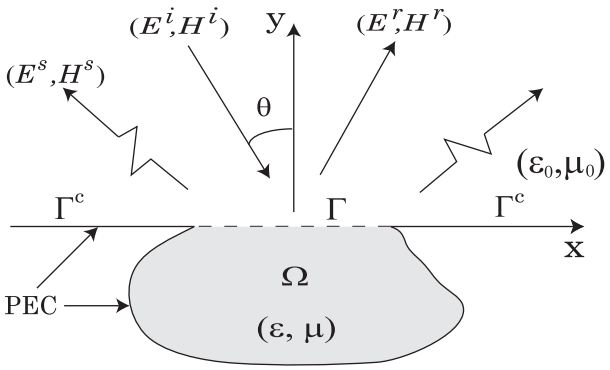

Figure 1. The geometry of cavity.

medium. In this setting, the electromagnetic scattering by the cavity is governed by the Helmholtz equation along with Sommerfeld's radiation conditions imposed at infinity. Because of its significant industrial and military applications, the cavity problem has attracted much attention. A variety of numerical methods including finite difference, finite element, boundary element methods, and hybrid methods have been developed by the engineering community for solving the open cavity problems [1–8]. A survey of numerical methods is presented in [9]. A detailed discussion and additional references may be found in Jin [10]. However, an unavoidable and fundamental question is how to solve the large-scale system of linear equations arising from electromagnetic scattering. Classical direct and iterative algorithms are not efficient especially for large cavity problems due to the indefinite nature of systems and high oscillation of solution.

This paper focuses on problems with large wave numbers and inhomogeneous media. The problem with large wave numbers, or more precisely with large 'ka' numbers, is of significant interest [3, 10, 11]. Here k is the wave number and a is the diameter of the computational domain. For electromagnetic cavity problems, microwaves are usually considered. Nonetheless, for large cavities, the large domain diameters give rise to high 'ka' numbers. The computation is especially challenging when the cavities are large compared with the wavelength of the fields due to the highly oscillatory nature of the fields. Numerical discretization for a large cavity problem results in an extremely large-scale indefinite system of linear equations. Recently a fast algorithm was proposed in [3] for solving the electromagnetic scattering from a rectangular cavity with a medium of x-directional homogeneous. The algorithm is based on the use of discrete Fourier transform in the horizontal direction and a Gaussian elimination in the vertical direction. Numerical experiments for large numbers of mesh points and large wave numbers show that the algorithm is efficient. In this paper, a preconditioning iterative algorithm is introduced for solving the electromagnetic scattering from a large cavity, in which a layered medium model is used as a preconditioner for the non-layered medium model. The fast algorithm developed in [3] is used for solving the cavity model of layered media.

Preconditioned iterative methods for solving electromagnetic scattering problems have been studied by many authors [12–14]. Most focus on Helmholtz models with some simple boundary conditions. Ernst and Golub [14] solved the interior Helmholtz model in a rectangular domain with impedance boundary conditions using preconditioning methods. They proposed several preconditioners including the discrete Helmholtz operators with Dirichlet or Neumann boundary conditions

DOI: 10.1002/nla

on two edges and a preconditioning Schur complement. Elman and O'leary [12] further studied the first preconditioner proposed in [14] and presented eigenvalue analysis for the preconditioned systems. Note that at each preconditioning iteration of their algorithm, one needs to solve the Helmholtz equation with Dirichlet or Neumann boundary conditions on two edges and impedance boundary conditions on the other two edges. Erlangga *et al.* [13] proposed a shifted-Laplace preconditioner for high wave number Helmholtz problems in heterogeneous media. A multigrid method is used to solve the preconditioner. For the cavity model, a preconditioning iterative method was proposed in [5], where the preconditioner is based on the Helmholtz model with Dirichlet boundary conditions on the wall of the cavity and an absorbing boundary condition on the aperture. At each iteration, one has to solve a cavity model with an absorbing boundary condition on the aperture.

The remainder of the paper is organized as follows. In Section 2, the model of a scattering problem from a cavity is formulated and further reduced to a bounded domain problem. Numerical discretization is addressed. A preconditioning algorithm is presented in Section 3 for the transverse magnetic (TM) case. Section 4 is devoted to numerical experiments of the algorithm.

2. THE ELECTROMAGNETIC CAVITY PROBLEM

We focus on a two-dimensional geometry by assuming that the medium and material are invariant in the z-direction. Assume also that the medium is non-magnetic and a constant magnetic permeability $\mu=\mu_0$ exists everywhere. The electromagnetic property of the medium is characterized by the dielectric coefficient ε, and $\mathrm{Im}(\varepsilon)\geqslant 0$.

Assume that a plane wave $u^{\mathrm{i}}=\mathrm{e}^{\mathrm{i}(\alpha x-\beta y)}$ is an incident wave on the cavity from the above, where $\alpha=k_0\sin\theta$, $\beta=k_0\cos\theta$, and $-\pi/2<\theta<\pi/2$ is the angle of incidence with respect to the positive y axis. Let u^{r} be the reflected wave. The relation between scattered field u^{s} and total field u can be expressed as

$$u^{\mathrm{s}}=u-u^{\mathrm{i}}-u^{\mathrm{r}} \tag{1}$$

Here we only consider the TM case, in which the magnetic field is transverse to the invariant direction and the time-harmonic Maxwell equations reduce to

$$\begin{aligned} \Delta u+k^2u &= f(x,y) \quad (x,y)\in\Omega\cup R_2^+ \\ u &= 0 \quad \text{on } \Gamma^C\cup\partial\Omega\backslash\Gamma \end{aligned} \tag{2}$$

together with the radiation boundary condition

$$\lim_{\mathrm{r}\to\infty}\sqrt{r}\left(\frac{\partial u^{\mathrm{s}}}{\partial r}-\mathrm{i}k_0u^{\mathrm{s}}\right)=0 \tag{3}$$

where R_2^+ denotes the upper-half space, $r=\sqrt{x^2+y^2}$, $k^2=\omega^2\varepsilon\mu=k_0^2\varepsilon_{\mathrm{r}}\mu_{\mathrm{r}}$, $\varepsilon_{\mathrm{r}}=\varepsilon/\varepsilon_0$ and $\mu_{\mathrm{r}}=\mu/\mu_0$ denote the relative permittivity and relative permeability, respectively, $\varepsilon_{\mathrm{r}}=\varepsilon_{\mathrm{r}}(x,y)$ in Ω and $k_0=\omega\sqrt{\varepsilon_0\mu_0}$ is the wave number in free space. The fields are said to be source free if the source term $f=0$.

Since the upper-half space is homogeneous, the so-called transparent boundary condition can be obtained by using either Green's function method (i.e. Hankel's function) [10] or the method of Fourier's transform [1, 2].

DOI: 10.1002/nla

In the TM case, the scattered field u^s satisfies

$$\begin{aligned} \Delta u^s + k_0^2 u^s &= 0 \quad (x, y) \in R_2^+ \\ u^s &= 0 \quad \text{on } \Gamma^C \\ u^s &= u(x, 0) \quad \text{on } \Gamma \end{aligned} \tag{4}$$

together with the radiation boundary condition (3) at infinite.

Let

$$G_d(\mathbf{x}, \mathbf{x}') = \frac{\mathrm{i}}{4}[H_0^{(1)}(k_0 r) - H_0^{(1)}(k_0 \bar{r})] \tag{5}$$

be the upper half-plane Dirichlet Green's function for the Helmholtz equation, which satisfies

$$\Delta G_d + k_0^2 G_d = -\delta(\mathbf{x}, \mathbf{x}'), \quad \mathbf{x}, \mathbf{x}' \in R_2^+ \tag{6}$$

$$G_d = 0 \quad \text{on } y = 0 \tag{7}$$

where $\mathbf{x} = (x, y)$, $\mathbf{x}' = (x', y')$, $r = |\mathbf{x} - \mathbf{x}'|$, $\bar{r} = |\mathbf{x} - \bar{\mathbf{x}}'|$, and $\bar{\mathbf{x}}' = x' - \mathrm{i}y'$ is the image of $\mathbf{x}$ with respect to the real axis. By Green's theory and the homogeneous boundary conditions,

$$\left.\frac{\partial u^s(\mathbf{x})}{\partial y}\right|_{y=0^+} = \frac{\mathrm{i}k_0}{2} \oint\!\!\!\!\!\!- _{\Gamma} \left[\frac{1}{|x - x'|} H_1^{(1)}(k_0|x - x'|) u^s(x', 0)\right] \mathrm{d}s(\mathbf{x}') \tag{8}$$

Substituting (1) into (8), we obtain

$$\left.\frac{\partial u}{\partial y}\right|_{y=0^+} = \frac{\mathrm{i}k_0}{2} \oint\!\!\!\!\!\!- _{\Gamma} \frac{1}{|x - x'|} H_1^{(1)}(k_0|x - x'|) u(x', 0)\, \mathrm{d}x' - 2\mathrm{i}\beta \mathrm{e}^{\mathrm{i}\alpha x}, \quad x \in (0, a) \tag{9}$$

where $\oint\!\!\!\!\!\!- _{\Gamma}$ denotes a Hadamard principle value (or finite part) integral (see [15, 16] and references therein). Define $g(x) = -2\mathrm{i}\beta \mathrm{e}^{\mathrm{i}\alpha x}$ and

$$I(u) := \frac{\mathrm{i}k_0}{2} \oint\!\!\!\!\!\!- _{\Gamma} \frac{1}{|x - x'|} H_1^{(1)}(k_0|x - x'|) u(x', 0)\, \mathrm{d}x' \tag{10}$$

The non-local boundary condition is given by

$$\frac{\partial u}{\partial n} = I(u) + g(x), \quad x \in (0, a) \tag{11}$$

where $n = (0, 1)$.

Since u satisfies the Helmholtz equation (2) and the transparent boundary condition (11), the total field u satisfies the following equation:

$$\begin{aligned} \Delta u + k^2 u &= f(x, y), \quad (x, y) \in \Omega \\ u &= 0 \quad \text{on } \partial\Omega \backslash \Gamma \\ \frac{\partial u}{\partial n} &= I(u) + g(x) \quad \text{on } \Gamma \end{aligned} \tag{12}$$

DOI: 10.1002/nla

Numerical approximations to the Helmholtz equation have been extensively investigated. For the sake of simplicity, we consider a simple five-point finite difference method for the discretization of the Helmholtz equation (12) with uniform meshes.

Let $\{x_i, y_j\}_{i,j=0}^{M+1,N+1}$ define a uniform partition of $\Omega=[-a/2, a/2]\times[-b, 0]$ with $x_{i+1}-x_i=h_x$ and $y_{j+1}-y_j=h_y$. Let v_{ij} be the finite difference solution at the point (x_i, y_j). The discrete finite difference system in the TM case can be given by

$$\frac{v_{i-1,j}-2v_{ij}+v_{i+1,j}}{h_x^2}+\frac{v_{i,j-1}-2v_{ij}+v_{i,j+1}}{h_y^2}+k_0^2\varepsilon_{\mathrm{r}_{ij}}v_{ij}=f_{ij}, \quad i=1,2,\ldots,M, \quad j=1,2,\ldots,N$$

where $\varepsilon_{\mathrm{r}_{ij}}=\varepsilon_{\mathrm{r}}(x_i, y_j)$ and $f_{ij}=f(x_i, y_j)$. In matrix form, we have

$$(A_x\otimes I_N+I_M\otimes A_y+D)v+(I_M\otimes a_{N+1})v_{N+1}=f \tag{13}$$

where $\otimes$ denotes the tensor product (Kronecker product), I_M is the $M\times M$ identity matrix,

$$A_x=\frac{1}{h_x^2}\,\mathrm{tridiag}(1,-2,1), \quad A_y=\frac{1}{h_y^2}\,\mathrm{tridiag}(1,-2,1) \tag{14}$$

$$D=k_0^2\,\mathrm{diag}(\varepsilon_{\mathrm{r}_{11}},\varepsilon_{\mathrm{r}_{12}},\ldots,\varepsilon_{\mathrm{r}_{1N}},\varepsilon_{\mathrm{r}_{21}},\ldots,\varepsilon_{\mathrm{r}_{2N}},\ldots,\varepsilon_{\mathrm{r}_{M1}},\ldots,\varepsilon_{\mathrm{r}_{MN}}) \tag{15}$$

$$a_{N+1}=\frac{1}{h_y^2}(0,\ldots,0,1)^{\mathrm{T}} \tag{16}$$

and

$$v=(v_{11},\ldots,v_{1N},v_{21},\ldots,v_{2N},\ldots,v_{M1},\ldots,v_{MN})^{\mathrm{T}}$$

$$v_j=(v_{1j},v_{2j},\ldots,v_{Mj})^{\mathrm{T}}$$

By using a backward finite difference scheme and a general approach for the non-local boundary condition, we obtain

$$\frac{v_{i,N+1}-v_{i,N}}{h_y}=\sum_{l=1}^{M}g_{il}v_{l,N+1}+g(x_i), \quad i=1,2,\ldots,M$$

i.e.

$$h_y^{-2}I_Mv_N+(h_y^{-1}G-h_y^{-2}I_M)v_{N+1}=-h_y^{-1}g \tag{17}$$

where $G=(g_{ij})_{i,j=1}^{M}$ is an $M\times M$ matrix.

The global system is given by

$$\begin{pmatrix}A & A_{12}\\ A_{21} & h_y^{-1}G-h_y^{-2}I_M\end{pmatrix}\begin{pmatrix}v\\ v_{N+1}\end{pmatrix}=\begin{pmatrix}f\\ -h_y^{-1}g\end{pmatrix} \tag{18}$$

where

$$A=A_x\otimes I_N+I_M\otimes A_y+D$$

$$A_{12}=I_M\otimes a_{N+1}$$

$$A_{21}=A_{12}^{\mathrm{T}}$$

DOI: 10.1002/nla

Numerical approximation to the Hadamard-type integral operator $I(u)$ has been studied by several researchers. We refer to [17–19] for details.

The major issue in computational electromagnetic scattering is to solve the system (18). When a large wave number and multi-medium are involved, the solution is oscillatory, and therefore a large number of mesh points are needed and a large-scale indefinite linear system is to be solved. In the following example, we present our numerical results for a simple cavity models where three Krylov subspace algorithms, GMRES(m) [20], Conjugate Orthogonal Conjugate Gradient method (COCG) [21], and BiCGstab [21], are used to solve the large-scale and ill-conditioning system (18), respectively. We will briefly discuss the iterative methods in Section 3.3. The iteration stops when the relative residual is less than $\delta = 10^{-5}$.

Example 2.1

We consider a simple cavity model: a plane wave scattering from a rectangular groove with 1 m wide and 0.25 m deep at normal incidence ($a = 1.0$ and $b = 0.25$). We assume that the groove is empty, i.e. $k = k_0$. Numerical results are shown in Table I for different k_0 and different mesh points, where m denotes the dimension of subspaces used in restarted GMRES method. The computational complexity and memory of GMRES(m) depend upon the dimension of subspace. We test GMRES(m) with $m = 10, 20, 30$ only for numerical comparison. One can see that all the three algorithms are not suitable for solving problems with large wave number, while COCG is relatively better, compared with other two algorithms. The number of iterations increase much as the number of mesh points or the wave number k_0 increases.

Table I. The number of matrix–vector products for empty cavity.

k_0	$M \times (N+1)$	m	GMRES(m)	COCG	BiCGstab
2π	19×5	10	69	27	40
		20	37		
		30	27		
	39×10	10	203	53	76
		20	131		
		30	88		
	79×20	30	342	104	152
4π	39×40	30	173	61	94
	79×20	30	437	119	192
6π	59×15	30	472	109	246
	119×30	30	1185	206	572
10π	99×25	30	1236	236	1754
	199×50	30	>2000	483	>2000
20π	199×50	30	>2000	991	>2000
	299×75	30	>2000	1497	>2000
30π	299×75	30	>2000	>2000	>2000
	399×100	30	>2000	>2000	>2000

DOI: 10.1002/nla

3. PRECONDITIONING ALGORITHMS

3.1. Fast algorithm for layered medium

For a layered medium, $\varepsilon_r = \varepsilon_r(y)$, a fast algorithm was proposed in [3]. The main idea of the fast algorithm is to generate a discrete Dirichlet-to-Neumann transform from the first equation of (18), i.e.

$$Av + A_{12} v_{N+1} = f$$

by a FFT-type algorithm, in which a fast Fourier transform is used in the horizontal direction and a forward Gaussian elimination is used in the vertical direction. Based on these two discrete Dirichlet-to-Neumann transforms from upper-half space and the cavity, respectively, (18) reduces to a system defined on the aperture of the cavity. A preconditioning BiCG iterative algorithm is applied for solving the resulting aperture system. For completeness, we present the fast algorithm and detailed implementation in this subsection.

For the tridiagonal Toeplitz matrix A_x, we have

$$S_M A_x S_M = \Lambda = \mathrm{diag}(\lambda_1, \lambda_2 \ldots \lambda_M)$$

where S_M denotes the discrete Fourier-sine transformation,

$$S_M = \sqrt{\frac{2}{M+1}} \left(\sin \frac{lm\pi}{M+1} \right)_{l,m=1}^{M}, \quad \lambda_l = -\frac{4(M+1)^2}{a^2} \sin^2 \frac{l\pi}{2(M+1)}$$

and $S_M^2 = I$.

By the discrete Fourier-sine transformation, we rewrite the discrete Helmholtz system (13) as

$$(\Lambda \otimes I_N + I_M \otimes A_y + I_M \otimes D_L)\bar{v} + (I_M \otimes a_{N+1})\bar{v}_{N+1} = \bar{f}$$

where

$$\bar{v} = (S_M \otimes I_N)v = (\bar{v}_{11}, \ldots, \bar{v}_{1N}, \bar{v}_{21}, \ldots, \bar{v}_{2N}, \ldots, \bar{v}_{M1}, \ldots, \bar{v}_{MN})^{\mathrm{T}}, \quad \bar{v}_{N+1} = S_M v_{N+1}$$

$$\bar{f} = (S_M \otimes I_N) f = (\bar{f}_{11}, \ldots, \bar{f}_{1N}, \bar{f}_{21}, \ldots, \bar{f}_{2N}, \ldots, \bar{f}_{M1}, \ldots, \bar{f}_{MN})^{\mathrm{T}}$$

$$D_L = k_0^2 \,\mathrm{diag}(\varepsilon_r(y_1), \varepsilon_r(y_2), \ldots, \varepsilon_r(y_N))$$

Reordering the unknowns and equations above, we obtain

$$(A_y + \lambda_i I_N + D_L)\hat{v}_i + a_{N+1}\bar{v}_{i,N+1} = \hat{f}_i, \quad i = 1, 2, \ldots, M \tag{19}$$

where

$$\hat{v}_i = (\bar{v}_{i1}, \bar{v}_{i2}, \ldots, \bar{v}_{iN})^{\mathrm{T}}$$

$$\hat{f}_i = (\bar{f}_{i1}, \bar{f}_{i2}, \ldots, \bar{f}_{iN})^{\mathrm{T}}, \quad i = 1, 2, \ldots, M$$

Using a forward Gaussian elimination method with a row partial pivoting for the system (19) gives a discrete Dirichlet-to-Neumann transform defined by

$$\alpha_i \bar{v}_{iN} + \beta_i \bar{v}_{i,N+1} = \tilde{f}_{iN}, \quad i = 1, 2, \ldots, M$$

DOI: 10.1002/nla

or equivalently

$$S_M D_\alpha S_M v_N + S_M D_\beta S_M v_{N+1} = S_M \tilde{f}_N \tag{20}$$

where

$$D_\alpha = \mathrm{diag}(\alpha_1, \alpha_2, \ldots, \alpha_M)$$

$$D_\beta = \mathrm{diag}(\beta_1, \beta_2, \ldots, \beta_M)$$

Eliminating v_N from Equations (17) and (20) gives the aperture system

$$D_\alpha S_M (I_M - h_y G) v_{N+1} + D_\beta S_M v_{N+1} = \tilde{f}_N + h_y D_\alpha S_M g \tag{21}$$

Solving the linear system (21) gives the solution v_{N+1} on the interface Γ. The rest of the unknowns can be obtained by solving the following systems:

$$(A_y + \lambda_i I_N + D_L)\hat{v}_i = \hat{f}_i - a_{N+1}\bar{v}_{N+1}, \quad i = 1, 2, \ldots, M \tag{22}$$

in which $\bar{v}_N = -h_y g + (I_M - h_y G) v_{N+1}$ may be used for those possible nearly singular systems.

The algorithm is given below.

Algorithm I

(i) Generate the matrix G.
(ii) Calculate $\bar{f} = (S_M \otimes I) f$ and $S_M g$.
(iii) Calculate the LU decomposition to get D_α and D_β by using the forward Gaussian elimination with a row partial pivoting.
(iv) Solve the system (21) for v_{N+1}.
(v) Solve the system (22) for the rest of the unknowns.

3.2. Preconditioning

The convergence rate of iterative methods depends on the spectral properties of the coefficient matrix. Hence, one may attempt to transform the linear system into one that has more favorable spectral properties. A preconditioner is a matrix that effects such a transformation. A general preconditioned system with a preconditioner M is defined by

$$M^{-1}Au = M^{-1}b \quad \text{or} \quad AM^{-1}y = b, \quad u = M^{-1}y$$

They are referred to as a left and a right preconditioning, respectively. In this paper, we will adopt the right preconditioning.

We are interested in a large cavity with more general media. The fast algorithm cannot be applied directly for solving such a problem. Here, we propose a preconditioning technique for cavities with non-homogeneous media. Let

$$A_{\varepsilon_r} u = b$$

be a discrete linear system for the cavity model with the non-homogeneous medium $\varepsilon_r(x, y)$. A simple physical model with a vertically layered medium is employed as a preconditioner of a non-homogeneous model. A preconditioned system is given by

$$A_{\varepsilon_r} A_{\bar{\varepsilon}_r}^{-1} y = b, \quad u = A_{\bar{\varepsilon}_r}^{-1} y \tag{23}$$

DOI: 10.1002/nla

where $\bar{\varepsilon}_r = \bar{\varepsilon}_r(y)$ denotes a vertically layered medium, dependent upon the distribution of $\varepsilon_r(x, y)$. Then $A_{\bar{\varepsilon}_r}$ corresponds to a layered cavity model. Numerical computation for the layered cavity model can be performed in terms of the fast algorithm mentioned above. The computational complexity of the fast algorithm is $O(MN \log M)$ for an $M \times N$ grid. See [3] for details. For preconditioning Krylov subspace methods, a sparse subspace technique [22] can be used. This can reduce the computational cost and storage considerably.

3.3. Krylov subspace methods

A Krylov subspace iterative method is based on the construction of subspace

$$\mathscr{K}_m(A, r_0) = \text{span}\{r_0, Ar_0, A^2 r_0, \ldots, A^{m-1} r_0\}$$

where $\mathscr{K}_m(A, r_0)$ is a subspace of dimension m. $r_0 = b - Au_0$ is the initial residual vector and u_0 is the initial solution. There exist a variety of Krylov subspace methods. See [20, 21] for the detailed discussion. Here, the system (23) is solved by three iterative algorithms, GMRES(m), BiCG, and BiCGstab.

In general, GMRES is the most robust method. However, it becomes impractical due to its extremely large memory requirement as the number of iterations increases. In order to overcome this disadvantage, a restarted GMRES has been proposed. But it is well known that its convergence becomes slow or stagnant since some information is lost when restarted. Thus, how to accelerate the restarted GMRES is important. There exist many accelerating techniques, for example, GMRES-E [23], GMRES-IR [24], GMRES-DR [25], and NGMRES [26]. In [27], Chapman and Saad discussed why deflated and augmented techniques work. In this paper, we also apply GMRES-IR method to the system (23).

Let $H_{m+1,m}$ be the upper Hessenberg matrix generated by the Arnoldi process and $H_{m,m}$ is obtained from $H_{m+1,m}$ by deleting its last row. Denote by (λ_i, φ_i) the eigenpairs of the generalized eigenvalue problem (GEP)

$$H^*_{m+1,m} H_{m+1,m} \varphi_i = \lambda_i H^*_{m,m} \varphi_i \tag{24}$$

$\{\lambda_i\}$ are called the harmonic Ritz values with respect to the subspace $\mathscr{K}_m(A, r_0)$, and

$$(z_1, z_2, \ldots, z_m) = V_m(\varphi_1, \varphi_2, \ldots, \varphi_m)$$

are called the corresponding harmonic Ritz vectors, where V_m is an $n \times m$ matrix with basis vectors produced by the Arnoldi process. In the GMRES-IR method, the Krylov subspace is defined by

$$\text{span}\{r_0, Ar_0, A^2 r_0, \ldots, A^{m-k-1} r_0, z_1, z_2, \ldots, z_k\}$$

We denote the algorithm by GMRES(m, k). Note that in this algorithm, only m–k matrix–vector products are needed in one restarted process. The implementation for this augmented subspace is more complicated. For more details refer to [24].

On the other hand, compared with GMRES, BiCG and BiCGstab need less storage. At each iteration, two matrix–vector products are needed for general matrices. When the matrix A is Hermitian positive definite, BiCG reduces to classical conjugate gradient method, for which only one matrix–vector product is used at each iteration. It has been noted [28–31] that the coefficient matrix A in many electromagnetic scattering problems, particularly for cavity problems governed by the Helmholtz equation [10], is complex symmetric, but not Hermitian. In this case, BiCG reduces

DOI: 10.1002/nla

to COCG method and requires only one matrix–vector product per iteration. For our problems, both the original matrix and the vertically layered medium preconditioner are complex symmetric, so COCG method can be used, i.e. only one matrix–vector product and one preconditioner solve are required per iteration. However, BiCGstab still requires two matrix–vector products and two preconditioner solves per iteration. We refer to [21] for the details on implementation of the COCG method and preconditioning COCG method.

4. NUMERICAL EXPERIMENTS

In this section, computational results are reported for several cavity models to test our preconditioning algorithm. We focus on the efficiency of the preconditioning algorithm for solving the system (23). Four Krylov subspace methods, COCG, BiCGstab, GMRES(m), and GMRES-IR, are applied. The initial guess x_0 is set to the zero vector. Throughout the paper, the computation is performed on a Blade 1000 Sun-workstation in double complex precision.

The physical parameter of interest is the radar cross section (RCS), which is defined by

$$\sigma = \frac{4}{k_0}|P(\phi)|^2$$

where ϕ is the observation angle with respect to the positive x-axis and P is the far-field coefficient given by

$$P(\phi) = \frac{k_0}{2}\sin\phi \int_\Gamma u e^{ik_0 x\cos\phi}\,dx$$

A commonly used error measure (e.g. see [5, 12, 13]) is

$$E_R = \frac{\|b - Au^p\|_2}{\|b\|_2}$$

where u^p is the numerical solution at the pth iteration. The iteration stops when $E_R \leqslant \delta$. Here we always choose $\delta = 10^{-5}$.

Example 4.1

We consider a cavity model with the same size as in Example 2.1, a rectangular groove 1 m wide and 0.25 m deep ($a = 1.0$ and $b = 0.25$). The preconditioning iterative method is tested against the cavity model with homogeneous and inhomogeneous media, respectively.

The cavity models filled with the homogeneous media $\varepsilon_r = 1.0$ and $\varepsilon_r = 4 + i$ are two standard test problems [10]. We apply the fast algorithm in Section 2 for solving these two model problems. Numerical results are obtained with 99 mesh points at each coordinate direction. The magnitude of the field on the aperture and the backscatter RCS are given in Figure 2, compared with results obtained in [10] by finite element method.

For inhomogeneous cases, we consider two different distributions of inhomogeneous media shown in Figure 3, denoted by Cavity I and Cavity II, respectively, where

$$\varepsilon_r = \begin{cases} \varepsilon_{r_0} & \text{in } \Omega/\Omega_1 \\ \varepsilon_{r_1} & \text{in } \Omega_1 \end{cases} \tag{25}$$

DOI: 10.1002/nla

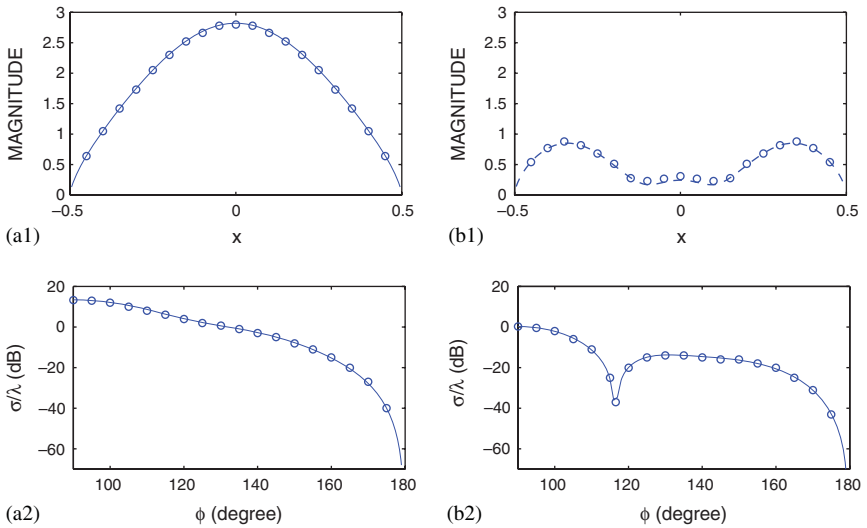

Figure 2. The magnitude of the aperture electric field at $\theta=0$ and backscatter RCS for $k_0=2\pi$: (a) $\varepsilon_r=1.0$ and (b) $\varepsilon_r=4+\mathrm{i}$ (o: numerical results in [10]).

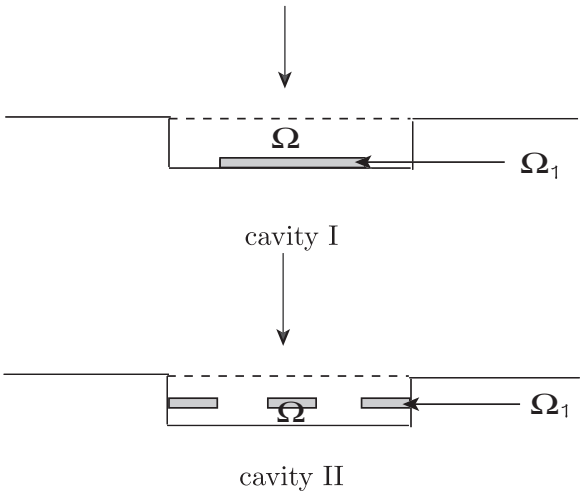

Figure 3. Two cavities of non-layered media.

We always assume that $k_0^2=\omega^2\varepsilon_0\mu_0$ and $k_1^2=k_0^2\varepsilon_{r_1}\mu_{r_1}=k_0^2\varepsilon_{r_1}$, where k_0 defines the wave number of the incident wave. See [15] for other cavity models and numerical experiments.

First, we apply our preconditioning iterative method for solving the cavity problems. Numerical results with COCG, BiCGstab, and GMRES(m) are presented in Tables II–IV. In Table II, we present the numbers of matrix–vector products of the preconditioning method for the model Cavity I with $\varepsilon_{r_1}=2.0$ and k_0 from the small wave number $k_0=2\pi$ to the large wave number $k_0=36\pi$.

DOI: 10.1002/nla

Table II. The number of matrix–vector products for cavity I with $\varepsilon_{r_1}=2.0$.

k_0	$M\times(N+1)$	m	GMRES(m)	COCG	BiCGstab
2π	39×10	10	3	3	4
	99×25	10	3	3	4
4π	59×15	10	4	4	6
	99×25	10	4	4	6
8π	99×25	10	7	7	8
	199×50	10	7	7	8
10π	299×75	10	8	9	12
	399×100	10	8	9	12
20π	299×75	10	29	18	26
		20	18		
	399×100	10	29	18	26
		20	18		
30π	399×100	20	99	38	100
		30	49		
	499×125	20	97	38	80
		30	49		
36π	399×100	20	>300	62	>300
		30	>300		
	499×125	20	>300	63	>300
		30	>300		

Table III. The number of matrix–vector products for cavity I.

k_0	ε_{r_1}	$M\times(N+1)$	m	GMRES(m)	COCG	BiCGstab
2π	2	99×25	10	3	3	4
	16	199×50	10	6	6	8
	50	299×75	10	14	12	32
		399×100	10	14	12	32
	100	399×100	10	170	19	72
			20	17		
		499×125	10	191	19	100
			20	17		
	$4+\mathrm{i}$	99×25	10	3	3	4
	$10+\mathrm{i}$	199×50	10	5	5	6
	$1+10\mathrm{i}$	199×50	10	4	4	6
	$50+\mathrm{i}$	299×75	10	14	12	24
	$50+10\mathrm{i}$	399×100	10	11	11	18
		499×125	10	11	11	18

The iteration stops when the error E_R is less than $\delta=10^{-5}$ or the number of matrix–vector products is larger than 300. We present in Figure 4 the magnitude of the aperture electric field and the backscatter RCS for the cavity I with the large wave number $k_0=30\pi$. Numerical results are obtained with a 400×100 mesh. One can see that the solution of cavity problems with large wave

DOI: 10.1002/nla

Table IV. The number of matrix–vector products for cavity II with $\varepsilon_{r_1} = 2.0$.

k_0	$M \times (N+1)$	m	GMRES(m)	COCG	BiCGstab
2π	39×10	10	3	3	4
	99×25	10	4	4	4
4π	59×15	10	6	6	8
	99×25	10	6	6	8
8π	99×25	10	8	9	10
	199×50	10	8	8	10
10π	299×75	10	8	9	12
	399×100	10	9	10	12
20π	399×100	10	39	26	32
		20	29		
	499×125	10	39	27	34
		20	28		
30π	399×100	20	198	52	100
		30	89		
	499×125	20	174	52	116
		30	87		
36π	399×100	20	274	83	202
		30	178		
	499×125	20	251	75	164
		30	167		

numbers is highly oscillatory. In Table III, we examine the same model with the incident wave of a small wave number $k_0 = 2\pi$ and different ε_{r_1}, including real and complex media. In Table IV, we present numerical results for cavity II, where $\varepsilon_{r_1} = 2.0$. To compare these Krylov algorithms, we present in Figure 5 the convergence history of GMRES(20), GMRES(30), COCG and BiCGstab for cavity I with $k_0 = 30\pi$ and $\varepsilon_{r_1} = 2.0$.

Next, we test the ILU preconditioning algorithms for cavity problems. Here ILU(0) retains the same sparse structure as the coefficient matrix and ILU(ε) needs to compute the incomplete LU factorization of a sparse matrix using the drop tolerance specified by the non-negative scalar ε. We refer to [20] for a more detailed discussion on incomplete LU preconditioners. We present numerical results obtained by the ILU preconditioning algorithms in Table V, where GMRES(m) and BiCGstab algorithms are used for solving the preconditioned system, respectively. Figure 6(a) shows the spectrum of the matrix for cavity I with wave number $k_0 = 10\pi$, $\varepsilon_{r_1} = 2.0$ and mesh 100×25. In Figure 6(b)–(d), we also provide the spectra of the preconditioned system proposed in this paper, the ILU(0) preconditioned system and the ILU(0.01) preconditioned system, respectively.

Several observations are in order:

- The new preconditioning method is very efficient for cavity models with $k_0 \leqslant 10\pi$. In this case, the preconditioned Krylov algorithms requires less than 10 iterations. For the cavity models with large wave numbers, the preconditioning iterative method needs more iterations while those non-preconditioning algorithms are not convergent in these cases (see Table I).

DOI: 10.1002/nla

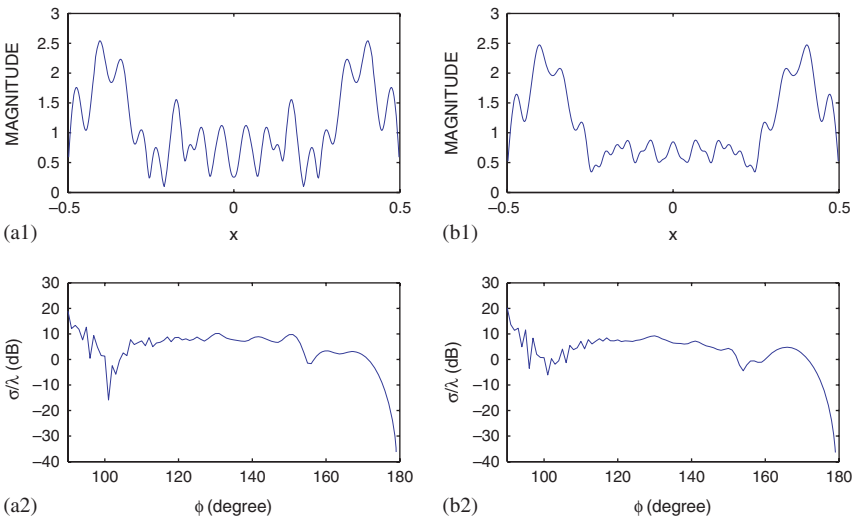

Figure 4. The magnitude of the aperture electric field at $\theta = 0$ and backscatter RCS for $k_0 = 30\pi$ for cavity I: (a) $\varepsilon_{r_1} = 2.0$ and (b) $\varepsilon_{r_1} = 4 + i$.

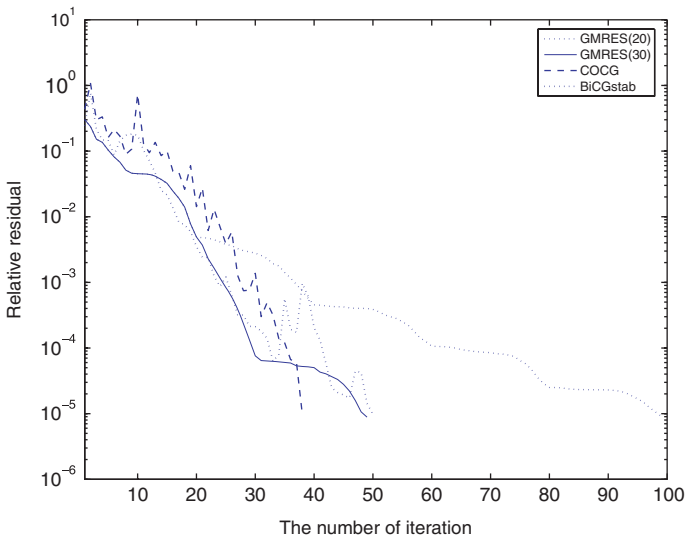

Figure 5. Performance of GMRES(20), GMRES(30), COCG and BiCGstab for cavity I with $k_0 = 30\pi$, $\varepsilon_{r_1} = 2.0$.

- In all cases, the number of iterations for all three iterative algorithms is independent of the number of mesh points used, but dependent upon the wave number, approximately proportional to k_0.

DOI: 10.1002/nla

Table V. The number of matrix–vector products (MATVEC) and CPU time (s) for cavity I with $\varepsilon_{r_1}=2.0,\ M=299, N+1=75$.

		GMRES(10)		BiCGstab	
k_0	Preconditioner	MATVEC	CPU	MATVEC	CPU
10π	ILU(0)	>1000	102.37	>1000	72.99
	ILU(0.01)	680	81.77	757	67.50
	Our method	8	2.47	12	3.27
20π	ILU(0)	>1000	107.74	>1000	74.30
	ILU(0.01)	>1000	125.02	>1000	90.16
	Our method	33	11.94	26	8.11

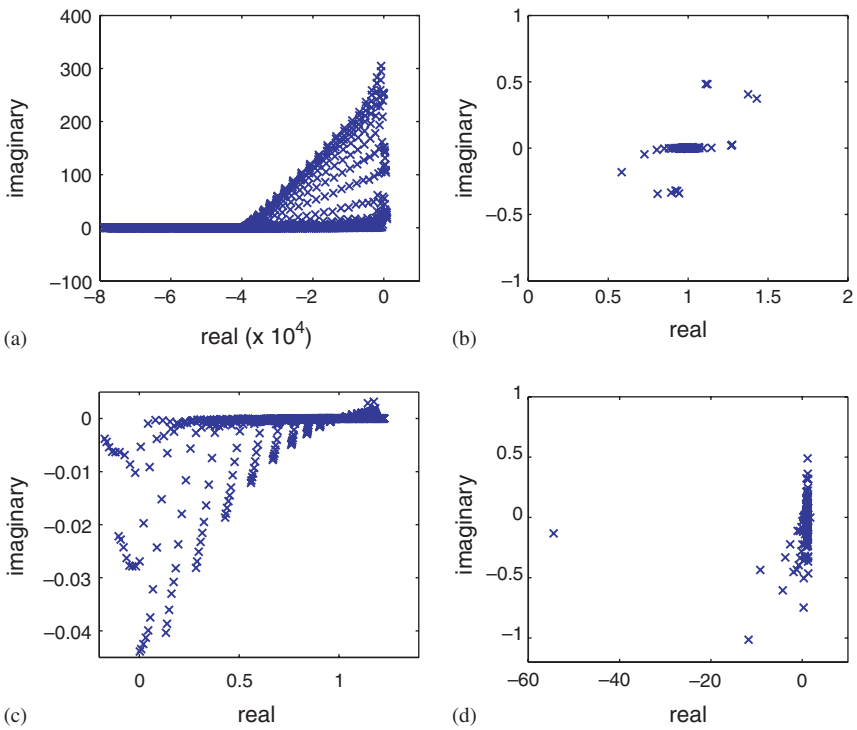

Figure 6. Spectrum of the matrix for cavity I with wave number $k_0=10\pi$ and grid 100×25: (a) original matrix; (b) vertically layered preconditioned matrix; (c) ILU(0) preconditioned matrix; and (d) ILU(0.01) preconditioned matrix.

- COCG requires less matrix–vector products than GMRES(m) in all cases. Also GMRES(m) needs more memory. For large wave numbers, COCG shows better performance. For example, in the case of $k_0=36\pi$, COCG is convergent within 63 iterations for the Cavity I, while GMRES(m) and BiCGstab are not convergent within 300 iterations.

DOI: 10.1002/nla

- It has been noted in many applications that GMRES(m) seems more stable. The residual of GMRES(m) iteration given in Figure 6 decreases monotonically, while BiCGstab iteration is less stable since the residual of BiCGstab iteration often jump up before the iteration stops. Moreover, our numerical experiments show that BiCGstab does not converge for some special initial guess $\tilde{r}$.
- ILU(0.01) algorithm requires less iterations than ILU(0), while it produces more non-zero entries in the incomplete LU factorization. However, both ILU(0) and ILU(0.01) algorithms require much more iterations than the proposed preconditioning algorithm. At each iteration, due to the Toeplitz structure of discrete non-local operator on aperture, our algorithm needs less operation counts. The new preconditioning method saves the CPU time remarkably. Also we can see from Figure 6 that all eigenvalues of our preconditioned system locate at the right half plane with a cluster at the point $(1, 0)$, while two ILU preconditioned systems are indefinite.

Finally, we apply the GMRES-IR algorithm for solving the cavity problems with large wave numbers. In Tables VI and VII, we show numerical results of three GMRES-IR algorithms, GMRES($m, 1$), GMRES($m, 3$), GMRES($m, 5$), compared with GMRES(m) for the two cavities

Table VI. The number of matrix–vector products of for cavity I with $\varepsilon_{r_1} = 2.0$.

k_0	$M \times (N+1)$	m	GMRES(m)	GMRES(m,1)	GMRES(m,3)	GMRES(m,5)
30π	399×100	15	185	192	108	70
		20	99	81	76	62
	499×125	15	178	168	84	72
		20	97	77	71	62
36π	399×100	20	>300	>300	290	150
		30	>300	142	110	84
	499×125	20	>300	>300	255	137
		30	>300	122	108	80

Table VII. The number of matrix–vector products for cavity II with $\varepsilon_{r_1} = 2.0$.

k_0	$M \times (N+1)$	m	GMRES(m)	GMRES(m,1)	GMRES(m,3)	GMRES(m,5)
30π	399×100	15	>300	252	98	94
		20	198	145	94	90
		30	89	84	76	73
	499×125	15	>300	248	99	91
		20	174	137	84	78
		30	87	72	74	67
36π	399×100	20	274	219	181	166
		30	178	118	131	121
	499×125	20	251	228	169	150
		30	167	144	129	105

DOI: 10.1002/nla

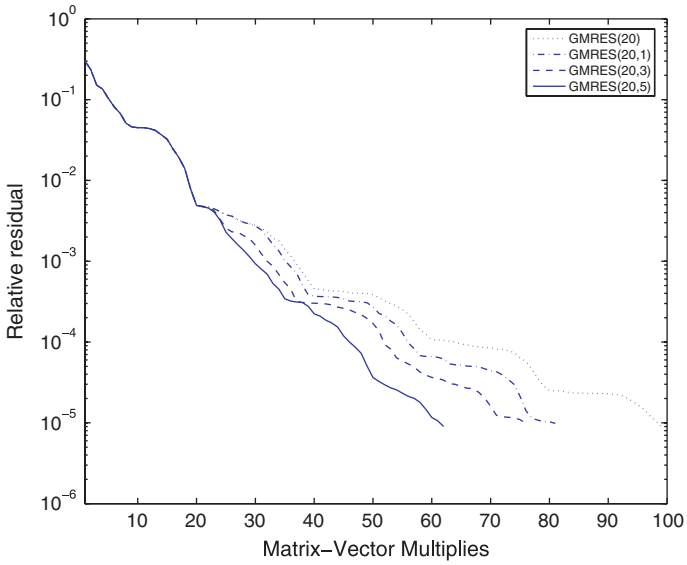

Figure 7. Performance of GMRES(20), GMRES(20,1), GMRES(20,3) and GMRES(20,5) for cavity I with $k_0 = 30\pi$, $\varepsilon_{r_1} = 2.0$.

with $k_0 = 30\pi$ and $k_0 = 36\pi$, respectively. Figure 7 shows the convergence history of GMRES(20), GMRES(20,1), GMRES(20,3), and GMRES(20,5) for cavity I with $k_0 = 30\pi$ and $\varepsilon_{r_1} = 2.0$. One can see that, compared with the GMRES(m), the GMRES-IR algorithms do accelerate the convergence in all cases and save the computational cost.

5. CONCLUSION

We have proposed a preconditioning algorithm for solving electromagnetic scattering from large cavities. No numerical investigations have been done for such large cavity problems, although preconditioning algorithms have been studied for many related artificial problems; Helmholtz equation with simple boundary conditions. The approximation to the cavity problem consists of two parts: discrete Helmholtz equation in the cavity and discrete non-local transparent boundary condition on the aperture. The former results in a sparse system and the latter produces a full Toeplitz system. The preconditioner proposed here is based on the same physical model with a layered medium. A fast algorithm developed in [3] is used for the preconditioner. The Toeplitz structure of discrete transparent boundary condition is taken into account. Three classical iterative algorithms, GMRES, COCG and BiCGstab, and harmonic Ritz vector techniques are used for solving the preconditioned system. Our numerical experiments show that the preconditioning algorithm proposed here is efficient for those large cavity models until $k = 36\pi$. The number of iterations is independent of the number of mesh points and dependent upon only the wave number. Moreover, compared with other two iterative algorithms, COCG algorithm seems more attractive and harmonic Ritz vector technique is able to speed up the convergence of GMRES algorithm.

DOI: 10.1002/nla

ACKNOWLEDGEMENTS

The authors would like to thank the referees for their valuable suggestions. The work was supported in part by a grant from the Research Grants Council of the Hong Kong Special Administrative Region, China (Project No. CityU 102204).

REFERENCES

1. Ammari H, Bao G, Wood A. An integral equation method for the electromagnetic scattering from cavities. *Mathematical Methods in the Applied Sciences* 2000; **23**:1057–1072.
2. Ammari H, Bao G, Wood A. Analysis of the electromagnetic scattering from a cavity. *Japan Journal of Industrial and Applied Mathematics* 2002; **19**:301–310.
3. Bao G, Sun W. A fast algorithm for the electromagnetic scattering from a cavity. *SIAM Journal on Scientific Computing* 2005; **27**:553–574.
4. Liu J, Jin JM. A special higher-order finite-element method for scattering by deep cavity. *IEEE Transactions on Antennas and Propagation* 2000; **48**:694–703.
5. Liu J, Jin JM. A highly effective preconditioner for solving the finite element-boundary integral matrix equation of 3-D scattering. *IEEE Transactions on Antennas and Propagation* 2002; **50**:1212–1221.
6. Ross DC, Volakis JL, Anastassiu HT. Hybrid finite element-modal analysis of jet engine inlet scattering. *IEEE Transactions on Antennas and Propagation* 1995; **43**:277–285.
7. Rousseau PR, Burkholder RJ. A hybrid approach for calculating the scattering from obstacles within large, open cavities. *IEEE Transactions on Antennas and Propagation* 1995; **43**:1068–1075.
8. Xiang Z, Chia TT. A hybrid BEM/WTM approach for analysis of the EM scattering from large open-ended cavities. *IEEE Transactions on Antennas and Propagation* 2001; **49**:165–173.
9. Anastassiu HT. A review of electromagnetic scattering analysis for inlets, cavities, and open ducts. *IEEE Antennas and Propagation Magazine* 2003; **45**:27–40.
10. Jin JM. *The Finite Element Method in Electromagnetics* (2nd edn). Wiley: New York, 2002.
11. Hawkins SC, Chen K, Harris PJ. On the influence of the wavenumber on compression in a wavelet boundary element method for the Helmholtz equation. *International Journal of Numerical Analysis and Modeling* 2007; **4**:48–62.
12. Elman H, O'Leary DP. Efficient iterative solution of the three dimensional Helmholtz equation. *Journal of Computational Physics* 1998; **142**:163–181.
13. Erlangga YA, Oosterlee CW, Vuik V. A novel multigrid based preconditioner for heterogeneous helmholtz problems. *SIAM Journal on Scientific Computing* 2006; **27**:1471–1492.
14. Ernst OG, Golub GH. A domain decomposition approach to solving the Helmholtz equation with radiation boundary condition. *Contemporary Mathematics* 1994; **157**:177–192.
15. Wang Y. Preconditioning iterative algorithms for electromagnetic scattering from large cavities. *Ph.D. Thesis*, City University of Hong Kong, 2007.
16. Wu J, Wang Y, Li W, Sun W. Toeplitz-type approximations to the Hadamard integral operators and their applications in electromagnetic cavity problems. *Applied Numerical Mathematics* 2008; **58**:101–121.
17. Sun W, Wu J. Newton–Cotes formulas for numerical evaluation of certain hypersingular integrals. *Computing* 2005; **75**:297–309.
18. Wu J, Sun W. The superconvergence of trapezoidal rule for Hadamard finite part integrals. *Numerische Mathematik* 2005; **102**:343–363.
19. Wu J, Sun W. The superconvergence of Newton–Cotes quadrature for Hadamard finite-part integrals on interval. *Numerische Mathematik* 2008; **109**:143–165.
20. Saad Y. *Iterative Methods for Sparse Linear Systems* (2nd edn). SIAM: Philadelphia, 2003.
21. van der Vorst HA. *Iterative Krylov Methods for Large Linear Systems*. Cambridge University Press: Cambridge, 2003.
22. Ito K, Toivanen J. Preconditioned iterative methods on sparse subspaces. *Applied Mathematical Letters* 2006; **19**:1191–1197.
23. Morgan RB. A restarted GMRES method augmented with eigenvectors. *SIAM Journal on Matrix Analysis and Applications* 1995; **16**:1154–1171.
24. Morgan RB. Implicitly restarted GMRES and Arnoldi methods for nonsymmetric systems of equations. *SIAM Journal on Matrix Analysis and Applications* 2000; **21**:1112–1135.

DOI: 10.1002/nla

25. Morgan RB. GMRES with deflated restarting. *SIAM Journal on Scientific Computing* 2002; **24**:20–37.
26. Niu Q, Lu L, Ng M. A new restarted GMRES using modified starting vector. Manuscript, 2006.
27. Chapman A, Saad Y. Deflated and augmented Krylov subspace techniques. *Numerical Linear Algebra with Applications* 1997; **4**:43–66.
28. van der Vorst HA, Melissen J. A Petrov–Galerkin type method for solving $Ax=b$, where A is symmetric complex. *IEEE Transactions on Magnetics* 1990; **26**:706–708.
29. Freund RW. Conjugate gradient-type methods for linear systems with complex symmetric coefficient matrices. *SIAM Journal on Statistical and Scientific Computing* 1992; **13**:425–448.
30. Clemens M, Weiland T. Iterative methods for the solution of very large complex-symmetric linear systems of equations in electrodynamics. In *Fourth Copper Mountain Conference on Iterative Methods*, *Part 2*, Copper Mountain, CO, U.S.A., Manteuffel TA, McCormick SF (eds). 1996.
31. Clemens M, Weiland T. Comparison of Krylov-type methods for complex linear systems applied to high-voltage problems. *IEEE Transactions on Magnetics* 1998; **34**:3335–3338.

DOI: 10.1002/nla